Nuclear Medicine and Molecular Imaging (2019) 53:253–262
https://doi.org/10.1007/s13139-019-00599-6

ORIGINAL ARTICLE

ISSN (print) 1869-3482
ISSN (online) 1869-3474

Utility of FDG-PET/CT for the Detection and Characterization of Sternal Wound Infection Following Sternotomy

Hadi Hariri[1] · Stéphanie Tan[1] · Patrick Martineau[2,3] · Yoan Lamarche[4] · Michel Carrier[4] · Vincent Finnerty[1] · Sébastien Authier[1] · Francois Harel[1] · Matthieu Pelletier-Galarneau[1,3]

Received: 9 April 2019 / Revised: 14 May 2019 / Accepted: 30 May 2019 / Published online: 14 June 2019

Abstract

Purpose FDG-PET/CT has the potential to play an important role in the diagnosis of sternal wound infections (SWI). The purpose of this study was to analyze the diagnostic accuracy of FDG-PET/CT for SWI in patients following sternotomy.

Methods We performed a single-center, retrospective analysis of patients who had undergone median sternotomy and FDG-PET/CT imaging. The gold standard consisted of positive bacterial culture and/or the presence of purulent material at surgery. Qualitative patterns of sternal FDG uptake, SUV_{max}, and associated CT findings were determined, and an imaging scoring system was developed. The diagnostic performances were studied in both the recent (≤ 6 months between sternotomy and imaging) and remote surgery phase (> 6 months).

Results A total of 40 subjects were identified with 11 confirmed SWI cases. Consensus interpretation was associated with a sensitivity of 91% and specificity of 97%. Combination of uptake patterns yielded an AUC of 0.96 while use of SUVmax yielded an AUC of 0.82.

Conclusions Results suggest that FDG-PET/CT may be useful for the diagnosis of SWI with optimal diagnostic accuracy achieved by identifying specific patterns of uptake. SUV_{max} can be helpful in assessing subjects with remote surgery, but its use is limited in the context of recent surgery. Further studies are required to confirm these results.

Keywords FDG-PET · Sternal wound infection · Infection imaging · Sternotomy

Introduction

Sternal wound infections (SWIs) are an infrequent but important source of morbidity and mortality following cardiac surgery [1], with early recognition and treatment associated with improved clinical outcomes [2]. Imaging plays an important role when sternal infection is suspected and can help distinguish between superficial (involving the skin,

✉ Matthieu Pelletier-Galarneau
matthieu.pelletier-galarneau@icm-mhi.org

Hadi Hariri
hadi.hariri@umontreal.ca

Stéphanie Tan
Steph_tan@hotmail.com

Patrick Martineau
pjmartineau@gmail.com

Yoan Lamarche
yoanlamarche@gmail.com

Michel Carrier
michel.carrier@icm-mhi.org

Vincent Finnerty
vincent.finnerty@icm-mhi.org

Sébastien Authier
sebastien.authier@icm-mhi.org

Francois Harel
francois_harel@hotmail.com

[1] Department of Medical Imaging, Institut de cardiologie de Montréal, Montreal, Quebec, Canada

[2] Department of Radiology, Health Sciences Centre, University of Manitoba, Winnipeg, Manitoba, Canada

[3] Gordon Center for Medical Imaging, Massachusetts General Hospital, Harvard Medical School, Boston, MA, USA

[4] Department of Surgery, Institut de cardiologie de Montréal, Montreal, Quebec, Canada

subcutaneous tissue, and/or pectoralis fascia) and deep (sternal osteitis and/or mediastinitis) SWI. This distinction is clinically relevant as each requires different management strategies and is associated with significantly different outcomes [3]. Currently, CT is often the initial imaging modality used to evaluate suspected SWI; however, despite the high sensitivity of CT for SWI [4], normal post-operative changes such as fluid collections, pericardial fluid, and subcutaneous emphysema can persist for several weeks following surgery, limiting its specificity [5–7]. As a result, distinguishing between an early focus of infection and residual post-operative changes can be challenging in the early post-operative period. In many centers, leukocyte scintigraphy is used as an adjunct to CT to help distinguish between post-operative changes and SWI. This technique offers high sensitivity and good specificity [8–10] but is limited by relatively poor image quality, the need to handle blood products, cost, and lengthy acquisition protocols.

The use of fluorodeoxyglucose (FDG) positron emission tomography/computed tomography (PET/CT) for infection imaging has evolved in recent years. Compared to traditional nuclear imaging techniques, FDG-PET/CT offers a shortened imaging protocol, improved spatial resolution, and excellent sensitivity for infection [11]. In particular, a recent meta-analysis has shown that FDG-PET/CT has higher sensitivity than conventional imaging with MRI and CT, as well as other scintigraphic techniques, for chronic osteomyelitis [12]. However, the use of FDG-PET/CT, particularly in the acute post-operative setting, is limited by the fact that inflammatory change can be a confounder for infection [13], limiting the specificity of the test.

The purpose of this retrospective study was to examine the diagnostic accuracy of FDG-PET/CT for SWI, to study patterns of FDG uptake to assist in the diagnosis of SWI by determining the imaging features which optimized diagnostic accuracy, and to examine the natural evolution of post-operative inflammatory changes at the sternotomy site.

Methods

Patient Population

This retrospective study was approved by our institutional review board, and the requirement to obtain informed consent was waived. Medical records of patients who underwent FDG-PET/CT at the Institut de cardiologie de Montréal between November 2014 and October 2017 were retrospectively reviewed. Those with incomplete studies and those imaged for evaluation of myocardial viability were excluded. Then, subjects were identified through review of our radiological information system using a keyword search ("stern*", "manubr*", "xyphoid*", and "wire*") of FDG-PET/CT reports. The PET/CT images and medical charts of the patients flagged with the keyword search were reviewed, and only those with prior history of sternotomy were included (Fig. 1). Subjects were subdivided into recent (≤ 6 months between sternotomy and imaging) or remote surgery (> 6 months between sternotomy and imaging) subgroups.

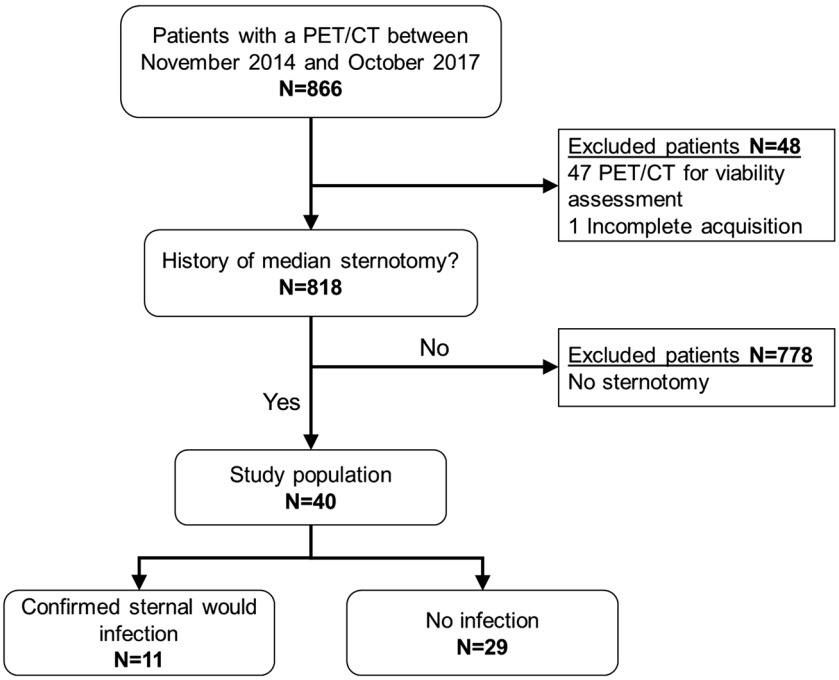

Fig. 1 Flowchart for subject enrolment

FDG-PET/CT Acquisition

Whole-body scans were performed on hybrid PET/CT scanner (Siemens Biograph mCT Flow 40 with TrueV, Knoxville, TN, USA). Following a fasting period of at least 6 h, approximately 370 MBq of ^{18}F-FDG was injected intravenously. Whole-body PET/CT images from the base of the skull to mid-thighs were acquired in 3D-mode between 45 and 75 min after tracer injection. PET images were reconstructed using ordered-subset expectation maximization (2 iterations and 21 subsets) algorithm with time of flight and point spread function modeling (ultraHD, Siemens). A 5-mm isotropic Gaussian filter was applied to the reconstructed images. Non-contrast CT was performed immediately after the PET acquisition using the following parameters: 120 kV, automated dose modulation (CARE Dose4D, Siemens) with a Quality Reference mAs of 70, total collimation width 19.2 mm, pitch 0.8, reconstructed slice thickness 3 mm, and B30f (medium smooth) convolution kernel.

FDG-PET/CT Interpretation

Images were reviewed independently by two certified nuclear medicine specialists (FH and MPG) using syngo.via VB20 software (Siemens Healthcare, Germany) who provided a gestalt interpretation. A certified radiologist with training in both cardiovascular imaging and musculoskeletal imaging (ST) provided additional interpretation of the CT portion of the PET/CT, without access to the PET portion of the study. PET/CT and CT image interpretation was performed with knowledge of the time interval between surgery and PET/CT imaging but blinded to all other clinical information. Disagreements were resolved by consensus. Interpretation made use of attenuation-corrected images and non-attenuation-corrected images in order to better assess for possible artifacts, particularly around sternal wires. Subjective assessment was performed using 5 predefined uptake patterns: (0) absent uptake, (1) low-grade diffuse sternal uptake, (2) high-grade diffuse sternal uptake (twice the liver activity or more), (3) focal sternal uptake (a dominant area of increased uptake not corresponding to a sternal wire), (4) focal uptake associated with a sternal wire, and (5) soft tissue uptake extending into the sternum (Fig. 2). Semi-quantitative analyses of FDG uptake (SUV_{max}) were performed using regions of interest (ROIs) drawn around the area with apparent maximal FDG uptake in the precordium on attenuation-corrected images. CT images were reviewed for the presence of subcutaneous emphysema, bone resorption, pneumomediastinum,

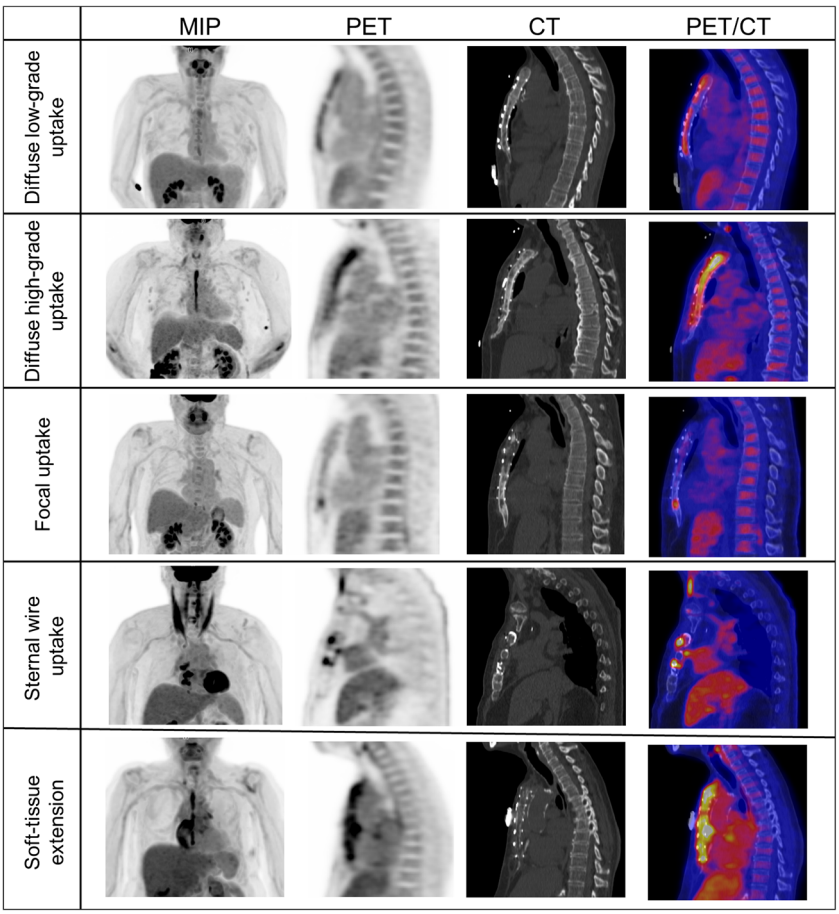

Fig. 2 Anterior maximal intensity projection (MIP) images as well as sagittal PET, CT, and fused PET/CT images of the FDG sternotomy uptake patterns

pericardial effusion, mediastinal edema, soft tissue collection, lymphadenopathy, mediastinal widening, and displaced wires.

Gold Standard

SWI was considered present in subjects with positive surgical drainage culture or positive culture from an excised wire. SWI was also considered present in the absence of a positive culture when purulent material was seen around the sternum or wires in subjects who underwent debridement. SWI was considered absent in those with negative surgical cultures and findings, in those who were referred for indications other than infection (e.g., oncology) without signs and symptoms of sternal infections, and in those subjects who did not undergo sternal debridement and did not show evidence of sternal infection in the 6 months following imaging.

Statistical Analysis

Categorical variables are presented as frequencies and continuous variables as mean ± SD with the exception of time interval between surgery and imaging which is presented as median (interquartile range). All statistical analyses were two-tailed, and a p value of < 0.05 was considered significant. Categorical variables were compared using Fisher's exact test when there were two categories and by chi-square tests when there were more than two categories. Continuous variables were compared with Student's two-sample t test with the exception of time interval between surgery and imaging which was compared using a non-parametric two-tailed Mann-Whitney test. The area under the receiver-operating characteristic (ROC) curve (AUC) was calculated and compared using the Hanley and McNeil method which allows comparison of AUC derived from the same dataset [14]. Optimal ROC thresholds were determined using Youden's index. Interobserver agreement on gestalt interpretation was evaluated using the kappa statistic. All analyses were performed using GraphPad Prism (GraphPad Prism version 6.01 for Windows, GraphPad Software, La Jolla California USA, www.graphpad.com) with the exception of the ROC analysis which was performed using MedCalc (MedCalc Statistical Software version 14.8.1, Ostend, Belgium; http://www.medcalc.org).

Results

Population Characteristics

A total of 866 patients underwent an FDG-PET/CT study at the Montreal Heart Institute between November 2014 and October 2017 (Fig. 1). Incomplete studies ($n = 1$) and subjects undergoing myocardial viability studies ($n = 47$) were excluded. Of the remaining 818 subjects, 40 (4.9%) had a history of

Table 1 Baseline characteristics of all included subjects. *BMI* body mass index, *CABG* cardiac artery bypass grafting, *LV* left ventricle

	All cases ($n = 40$)	Confirmed infection ($n = 11$)	No infection ($n = 29$)	p value
Age ± SD (years)	65 ± 14	70 ± 13	63 ± 14	0.23
Female (n, %)	11(27.5)	3 (27.3)	8 (27.6)	> 0.99
BMI (kg/m^2)	28.3 ± 5.2	28.2 ± 5.9	28.2 ± 4.8	0.93
Time since sternotomy (months)	32.6 ± 60.4	6.6 ± 6.8	42.4 ± 68.2	0.09
Surgery (n, %)				
CABG	16 (40.0)	7 (63.6)	9 (31.0)	0.19
Valve replacement	8 (20.0)	2 (18.2)	6 (20.7)	
Heart transplant	5 (12.5)	1 (9.1)	4 (13.8)	
LV aneurysm repair	1 (2.5)	1 (9.1)	0	
CABG and valve replacement	7 (17.5)	0	7 (24.1)	
Ross procedure	1 (2.5)	0	1 (3.4)	
Aortic surgery	2 (5.0)	0	2 (6.9)	
PET/CT indication (n, %)				
Suspicion of sternal infection	9 (22.5)	9 (81.8)	0	< 0.0001
Suspicion of other infection	18 (45.0)	2 (18.2)	16 (55.2)	
Oncology	10 (25.0)	0	10 (34.5)	
Vasculitis	3 (7.5)	0	3 (10.3)	

Table 2 Characteristics of subjects with confirmed sternal wound infection. Imaging features: (a) focal uptake; (b) sternal wire uptake; (c) soft tissue extension; (d) osseous resorption; (e) subcutaneous emphysema; (f) diffuse, high-grade uptake. *CRP* C-reactive protein, *WBC* white-blood cells

Subject ID	Age (years)	Sex	Time since surgery	CRP (mg/L)	WBC ($\times 10^9$/L)	SUV_{max}	Imaging features	PET/CT Score	Cultured bacteria
1	81	M	2 years	–	7.6	8.5	a, b, c, d	4	*S. aureus*
2	75	M	6 months	6.39	6.3	9.1	d, e, f	3	*S. epidermidis*
3	84	F	1 year	26.5	11.6	10.2	a, b, c, d, e	5	*S. aureus*
4	59	M	1 year	–	–	7.0	a, b, c, d, e	5	*S. epidermidis*
5	56	M	3 weeks	28.20	5.5	7.1	a, b, c, d	4	*S. epidermidis*
6	80	M	3 weeks	56.60	7.5	7.4	f	1	*C. koseri* and *S. marcescens*
7	69	M	5 months	9.43	7.4	8.5	a, b, c, d	4	*S. aureus*
8	74	F	7 months	–	8.6	8.5	a, b, d	3	None–purulent material on wires at surgery
9	81	M	1 month	38.00	6.0	9.0	a, b, c, d	4	*S. aureus*
10	67	M	1 month	–	6.2	6.5	a, b, c, d	4	*S. aureus*
11	40	F	5 months	43.6	8.6	11.3	a, c, e	3	*S. aureus*

sternotomy, identified through review of the PET/CT. Of these, 11 (27.5%) had a history of SWI, confirmed through review of the subject's medical record. The remaining 29 (72.5%) had no clinical history or findings to suggest sternal infection. Baseline characteristics of the subject population are presented in Table 1. Characteristics of subjects with confirmed sternal infection are presented in Table 2.

Subjects underwent PET/CT imaging 6.4 months (38.8) following sternotomy. Subjects without sternal infection underwent PET/CT imaging 9.0 months (45.3) (range 8 days to 21.2 years) following surgery while those with confirmed sternal infection were imaged 5.6 months (9.9) (range 19 days to 24.9 months) after surgery. The median delay between surgery and imaging was greater in non-infected subjects compared to subjects with confirmed infection but the difference did not reach statistical significance ($p = 0.10$). Twenty-one subjects (7 with sternal infection and 14 without sternal infection)

Table 3 Sternotomy site imaging findings on PET/CT. Low-grade and high-grade uptake are defined as below and above 2 × mean liver uptake, respectively

Imaging findings	Total ($n = 40$)	Infected ($n = 11$)	Non-infected ($n = 29$)	p value
FDG patterns of uptake				
Mean SUV_{max} ± SD	6.4 ± 3.6	8.5 ± 1.5	5.6 ± 3.9	0.024
Diffuse, high-grade uptake	12 (30%)	2 (18%)	10 (34%)	0.33
Focal activity	11 (28%)	9 (82%)	2 (7%)	< 0.0001
Sternal wire uptake	11 (28%)	8 (73%)	3 (10%)	< 0.0001
Diffuse, low-grade uptake	11 (28%)	0 (0%)	11 (38%)	0.015
Soft tissue extension	8 (20%)	8 (73%)	0 (0%)	< 0.0001
No significant uptake	5 (13%)	0 (0%)	5 (13%)	0.15
CT findings				
Osseous resorption	16 (40%)	10 (91%)	6 (21%)	< 0.0001
Mediastinal edema	16 (40%)	7 (64%)	9 (31%)	0.08
Widened mediastinum	9 (23%)	5 (46%)	4 (14%)	0.08
Lymphadenopathy	8 (20%)	2 (18%)	6 (21%)	1.0
Pericardial effusion	6 (15%)	2 (18%)	4 (14%)	1.0
Collection	6 (15%)	4 (36.4%)	2 (7%)	0.04
Displaced wire	6 (15%)	1 (9%)	5 (17%)	0.66
Pneumomediastinum	4 (10%)	1 (9%)	3 (10%)	1.0
Subcutaneous emphysema	3 (7.5%)	3 (27%)	0 (0%)	0.017

Table 4 Diagnostic performances of individual PET and CT imaging findings

Imaging features	OR (95%CI)	*p* value	Sensitivity (95%CI)	Specificity (95%CI)
PET findings				
[a]Soft tissue extension	143.3 (6.7–3055.6)	0.002	72.7 (39.0–94.0)	100 (88.1–100)
[a]Focal uptake	60.8 (7.4–496.2)	0.0001	81.8 (48.2–97.7)	93.1 (77.2–99.2)
[a]Sternal wire uptake	23.1 (3.9–137.8)	0.0006	72.7 (39.0–94.0)	89.7 (72.6–97.8)
[a]Diffuse high-grade uptake	0.4 (0.08–2.3)	0.3	81.8 (48.2–97.7)	34.5 (17.9–54.3)
Absent/diffuse low-grade uptake	0.04 (0.002–0.7)	0.03	0.0 (0.0–28.5)	55.1 (35.7–73.6)
CT findings				
[a]Osseous resorption	38.3 (4.1–361.3)	0.001	90.9 (58.7–99.8)	79.3 (60.3–92.0)
[a]Subcutaneous emphysema	24.3 (1.1–518.1)	0.04	27.3 (6.0–61.0)	100 (88.1–100)
Collection	23.3 (2.2–237.7)	0.008	36.4 (10.9–69.2)	93.1 (77.2–99.2)
Widened mediastinum	10.4 (1.9–56.0)	0.006	45.5 (16.8–76.6)	86.2 (68.3–96.1)
Mediastinal edema	3.9 (0.9–16.7)	0.07	63.6 (30.8–89.1)	69.0 (49.2–84.7)
Pericardial effusion	3.3 (0.5–19.4)	0.2	18.2 (2.3–51.8)	86.2 (68.3–96.1)
Pneumomediastinum	3.0 (0.4–24.5)	0.3	9.1 (0.2–41.3)	89.7 (72.7–97.8)
Displaced wire	1.4 (0.2–8.9)	0.7	9.1 (0.2–41.3)	82.8 (64.2–94.2)
Lymphadenopathy	0.9 (0.1–5.0)	0.9	18.2 (2.3–51.8)	79.3 (60.3–92.0)

[a] Imaging findings included in the scoring system

were imaged within 6 months of surgery and included in the recent surgery subgroup while 19 (4 with sternal infection) were imaged > 6 months after surgery and were included in the remote surgery subgroup.

Imaging Findings

An overview of the PET/CT findings at the sternotomy site in infected and non-infected subjects is shown in Table 3. The most frequently seen pattern of FDG uptake was diffuse high-grade uptake, present in 12 (30%) of subjects. Diffuse, low-grade uptake (mean SUV_{max} 3.7 ± 0.9) was reported in 11 subjects (28%), none of which had findings of infection. There was an absence of uptake noted in 5 (12.5%) subjects, all of which were imaged > 3 years following surgery and none having clinical findings of SWI. Conversely, sternal wire uptake, soft tissue uptake extending into the sternum, and focal uptake were predictors of SWI (Table 4). CT findings predictor of SWI included subcutaneous emphysema, widened mediastinum, soft tissue collection, and osseous resorption (Table 4).

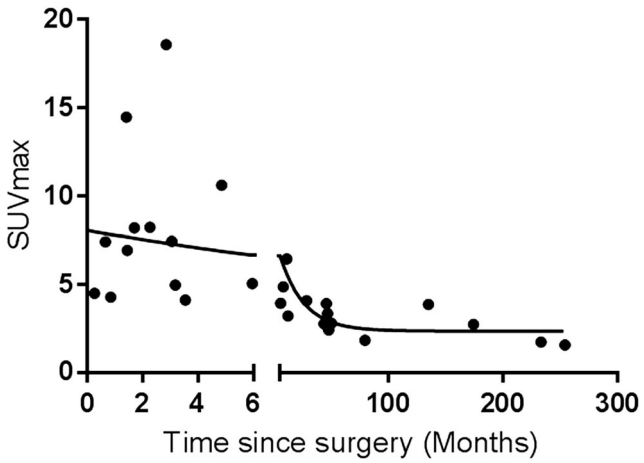

Fig. 3 Relationship between sternal SUV_{max} in non-infected patients as a function of time since sternotomy

Post-Operative Sternal FDG Uptake

In order to determine the normal evolution of sternal uptake post-surgery, the SUV_{max} from the non-infected subjects was modeled as a function of time using a one-phase exponential decay model. Analysis resulted in a decay half-life of 1.3 years and an R^2 of 0.37. Results are shown in Fig. 3. In the early period following surgery (< 6 months), normal sternal uptake was highly variable: non-infected subjects demonstrated SUV_{max} ranging from 3.2 to 18.6. Results conformed more closely to the model in the remote surgery subgroup (> 6 months) with SUV_{max} ranging from 1.6 to 6.5.

Diagnostic Accuracy

Consensus interpretation of PET/CT findings by two expert readers yielded an accuracy of 94% (95%CI 81–99%) with a sensitivity/specificity of 91% (95%CI 59–100%)/97% (95%CI 82–100%) for the diagnosis of SWI compared to gold

Table 5 Two-by-two diagnostic tables for the diagnosis of sternal wound infections using the gestalt PET/CT interpretation, CT-alone interpretation, and interpretation based on a SUVmax cutoff of 6.5 LAYOUT OF this table is somewhat confusing. COnsider adding horitontal lines between the 3 main rows (PET/CT, CT alone, SUVmax). Also, to help the readibility, we should add the word "totals" under each "No infection". I attached an uptdated version of the table to illustrate that. Thanks.

		Reference standard		
		Infection	No infection	Totals
PET/CT	Infection	10	1	11
	No infection	1	28	29
		11	29	40
CT alone	Infection	11	6	17
	No infection	0	23	23
		11	29	40
SUV_{max}	Infection	11	9	20
	No infection	0	20	20
		11	29	40

standard (Table 5). On the other hand, diagnosis based solely on CT features had an accuracy of 90% (95%CI 76–97%) with a sensitivity/specificity of 100% (95%CI 72–100%)/79% (95%CI 60–92%) (Table 5). In the recent surgery subgroup, consensus interpretation of PET/CT yielded an accuracy of 93% (95%CI 73–99%) with a sensitivity/specificity of 86% (95%CI 42–100%)/100% (95%CI 77–100%), while diagnosis based solely on CT features had an accuracy of 86% (95%CI 64–97%) with a sensitivity/specificity of 100% (95%CI 59–100%)/71% (95%CI 42–92%). In the remote surgery subgroup, consensus interpretation of PET/CT yielded an accuracy of 97% (95%CI 77–100%) with a sensitivity/specificity of 100% (95%CI 40–100)/93% (95%CI 68–100%), while diagnosis based solely on CT features had an accuracy of 93% (95%CI 72–100%) with a sensitivity/specificity of 100% (95%CI 40–100%)/87% (95%CI 60–98%). The differences in accuracy, sensitivity, and specificity between PET/CT and CT interpretation for all subjects were not statistically significant ($p > 0.25$). Furthermore, diagnostic accuracy, sensitivity, and specificity of PET/CT were not significantly different between the recent and remote surgery subgroups ($p > 0.9$). Interobserver agreement was very good with $\kappa = 0.87$ (95%CI 0.69–1.00). There was disagreement in only two cases, one case in the recent surgery subgroup and one case in the remote surgery subgroup.

Semi-Quantitative Analyses

Overall, SUV_{max} at the sternotomy site was higher in infected subjects compared to non-infected subjects (8.5 ± 1.4 vs 5.5 ± 3.8, $p = 0.02$, Fig. 4). In the remote surgery subgroup, SUV_{max} at the sternotomy site was also significantly higher in infected subjects compared to non-infected subjects (8.5 ± 1.3 vs 3.3 ± 1.3, $p < 0.0001$); however, in the recent surgery subgroup, the difference was no longer significant (8.4 ± 1.6 vs 7.8 ± 4.4, $p = 0.72$). Overall, ROC analysis of SUV_{max} yielded an AUC of 0.82 ± 0.07 (95%CI 0.67–0.93, $p < 0.0001$) with a sensitivity of 100% and specificity of 69% at a cutoff of 6.5 (Table 5). Within the recent surgery subgroup, ROC analysis of SUV_{max} yielded an AUC of 0.66 ± 0.12 (95%CI 0.43–0.85, $p = 0.18$) while, for the remote surgery subgroup, AUC was 0.95 ± 0.05 (95%CI 0.85–1.0, $p = 0.007$).

PET/CT Imaging Score

The impact on diagnostic accuracy of combinations of imaging features was considered by the introduction of an ad hoc imaging score relying exclusively on qualitative imaging features for PET/CT. The scoring system was defined as follows: the presence of individual imaging features (Table 4) within a study was assigned one point, with the overall score equivalent to the number of imaging features present. The diagnostic performance of the scoring system is reviewed in Table 6. ROC analysis of the PET/CT score yielded an AUC of 0.96

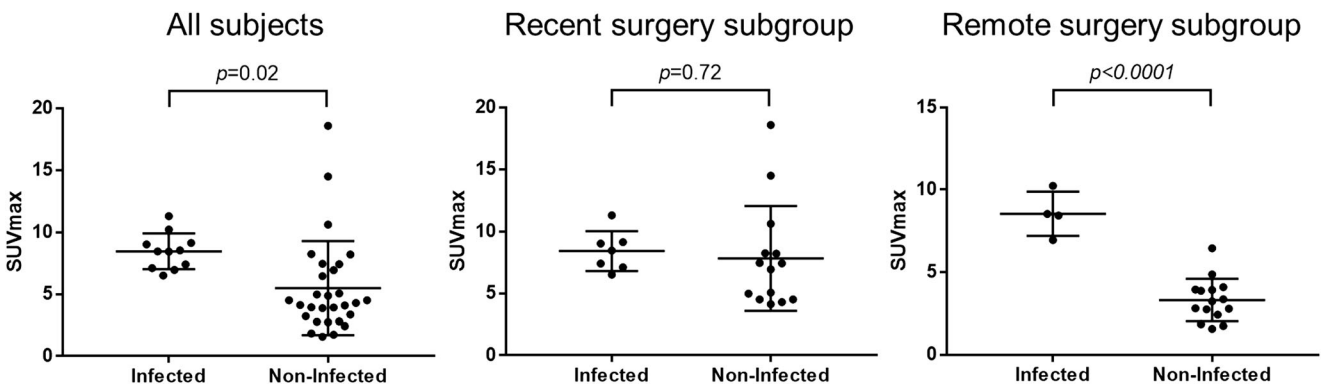

Fig. 4 Distribution of SUV_{max} in the infected and non-infected subjects, as well as in both the recent (≤ 6 months) and remote (> 6 months) surgery subgroups

Table 6 Diagnostic performance of PET/CT imaging score for the diagnosis of sternal wound infection. The performance of the imaging score is shown overall, as well as for the acute and chronic subgroups

Score	AUC (95%CI)	Sensitivity % (95%CI)	Specificity % (95%CI)
All	0.96 (0.85–1.0)		
1		100 (71.5–100)	51.7 (32.5–70.6)
2		90.9 (58.7–99.8)	79.3 (60.3–92.0)
3		90.9 (58.7–99.8)	96.6 (82.2–99.9)
4		63.6 (30.8–89.1)	100 (88.1–100)
5		18.2 (2.3–51.8)	100 (88.1–100)
Acute	0.91 (0.70–0.99)		
1		100 (59.0–100)	21.4 (4.7–50.8)
2		85.7 (42.1–99.6)	64.3 (35.1–87.2)
3		85.7 (42.1–99.6)	92.9 (66.1–99.8)
4		57.1 (18.4–90.1)	100 (76.8–100)
Chronic	1.0 (0.82–1.0)		
1		100 (39.8–100)	80.0 (51.9–95.7)
2		100 (39.8–100)	93.3 (68.1–99.8)
3		100 (39.8–100)	100 (72.2–100)

± 0.03 (95%CI 0.85–1.00, $p < 0.0001$). When limited to the recent surgery subgroup, ROC analysis of the imaging score yielded an AUC of 0.91 ± 0.08 (95%CI 0.70–0.99, $p < 0.0001$). ROC analyses of the imaging score in remote surgery subgroup yielded an AUC of 1.0 ± 0.0 (95%CI 1.0–1.0, $p < 0.003$). The AUCs of SUV_{max} were lower compared to those of imaging score but the difference did not reach statistical significance for all subjects ($p = 0.07$), recent surgery ($p = 0.08$), and remote surgery subgroup ($p = 0.32$).

Discussion

The results of this study suggest that FDG-PET/CT demonstrates excellent accuracy for the diagnosis of postoperative SWI and can differentiate between normal postsurgical changes from infectious changes with high sensitivity and high specificity. To our knowledge, this is the first study to evaluate the diagnostic performance of different imaging patterns of FDG-PET/CT and to propose simple imaging criteria, combining PET and CT findings, to assist in the diagnosis of SWI. Finally, this is the first study to report on the natural evolution of post-operative inflammatory changes at the sternotomy site.

The literature on the PET assessment of SWI is quite limited. The potential utility of FDG-PET/CT for characterizing sternal infections post sternotomy has previously been alluded to in a small case series [15]. More recently, a retrospective study suggested that PET is an accurate and useful modality for the assessment of SWIs [16]. This study reported an excellent sensitivity of 98.4% with a moderate specificity of 77.8% for sternal osteomyelitis. However, along with other issues, this study was limited by a lack of controls: of the 73 subjects included in the study, 72 were diagnosed with a SWI including mediastinitis, sternal osteomyelitis, costochondritis, and vascular graft infection. An even more significant limitation was that PET interpretation employed relied solely on the degree of FDG uptake in order to identify sites of infection, which likely accounts for the relatively low specificity reported. It is well known that inflammation is an important confounder when assessing infection with PET and that this is a particular concern at sites of previous surgical instrumentation where there is active formation of granulation tissue and scarring, as well as the influx of inflammatory cells, fibroblasts, and myofibroblasts, all of which are associated with increased FDG uptake, even in the absence of a septic process [17]. In this context, reliance on SUV alone has been shown to be particularly limited in distinguishing between infection and inflammation, particularly in the early post-operative phase [13, 18, 19]. Another important factor limiting the use of a fixed uptake threshold is that SUV measurements can be affected by several factors, both technical and biological, limiting the usefulness of universal diagnostic thresholds. Normalization of uptake intensity with respect to a reference tissue (such as lung or liver parenchyma) can be used but is also subject to limitations.

Much of what is currently known about the use of FDG-PET/CT for assessing postsurgical infections arises from the study of peri-prosthetic infections, with the best-studied being infections associated with orthopedic hardware. In that application, much attention has been placed on the particular pattern of FDG uptake as opposed to uptake intensity, and it has been shown that diagnosis based on the distribution of FDG uptake can

be highly accurate [20], while the use of SUV for diagnosis has met with limited success [11, 21, 22]. Another important lesson learned from this application is that diagnostic performance varies considerably with the particular diagnostic criteria employed [21–23]. The results of our study are consistent with these findings. Although FDG uptake intensity was, on average, greater in infected subjects, SUV_{max} alone could not reliably distinguish infection from normal postsurgical changes in the acute post-operative period, which is when most SWI occurs [1]. The fact that the difference in sternal uptake in those imaged within 6 months of sternotomy was not significant suggests that underlying post-operative inflammatory change and/or increased metabolism associated with healing can persist for a long time following surgery. Recognition of this fact is important as it represents a potential source of false-positive studies. Our results show that inflammatory changes and healing are usually associated with diffuse, low-grade uptake. However, several non-infected subjects demonstrated elevated FDG uptake in sternum, highlighting the limitation of using SUV cut-offs for diagnosis. Examining those subjects without infection revealed that, in the acute post-operative period, the intensity of uptake varied greatly and overlapped considerably with those subjects with documented sternal infection. This likely accounts for the low specificity of SUV_{max} thresholds to detect SWI early after surgery. In the remote surgery subgroup, uptake in non-infected subjects followed an exponential decay and, in certain cases, increased uptake persisted for decades after surgery. Nonetheless, differences between septic and aseptic uptake was significant in this context, suggesting that absolute uptake can play a role in the diagnosis of SWI several months after surgery.

In order to circumvent the limitations of uptake intensity for the diagnosis of postsurgical infections, we have determined multiple patterns of FDG uptake present in SWI. Comparison to pathology results confirms that these patterns are individually associated with good diagnostic accuracy. The results of this study suggest that very good diagnostic accuracy is possible when multiple patterns are present or when these patterns are used in conjunction with CT findings. While our results support that a gestalt interpretation can be highly accurate, we envision that the PET/CT score may be of use to more junior interpreters, or at those centers in which SWIs are less commonly seen.

In the acute setting, both the use of a gestalt interpretation and the proposed scoring system yielded higher accuracy, sensitivity, and specificity compared to diagnosis based on a SUV_{max} threshold alone, despite the small sample size of this study. Our results support that, as in the case of infected orthopedic hardware, the specific pattern of uptake is more useful than the actual degree of uptake in distinguishing infection from inflammation. In the remote surgery setting, the utility of SUV_{max} for the diagnosis of SWI increased with accuracy comparable to that of the gestalt interpretation and PET/CT score. Given that most SWI occurs early after surgery, the overall accuracy of SUV_{max} for the diagnosis of SWI was inferior to that of gestalt interpretation and the proposed scoring system.

CT is typically the initial imaging modality used to assess patients with suspected SWI. CT has been shown to be very sensitive for the detection of SWI, but its specificity can be limited by persistent postsurgical changes mimicking infection [5–7, 16], particularly in the recent surgery setting. Our results are consistent with this, with CT showing a specificity of 71% in subjects with acute infections. Interestingly, the use of FDG patterns resulted in greater specificity compared to CT interpretation and the use of SUV_{max} thresholds. FDG-PET/CT is often thought of as a test with high sensitivity but low specificity. While this is likely related to the use of uptake intensity cutoffs to establish diagnosis rather than uptake distribution patterns, this study suggests that interpretation based on imaging patterns can provide excellent sensitivity without sacrificing specificity in both recent and remote surgery settings.

Several limitations of this study need to be acknowledged. This was a retrospective study and is subject to the limitations inherent to that study design. In addition, the number of subjects with SWIs was quite small limiting the statistical power of the analyses. The prevalence of SWI in our population was quite high compared to reported rates in the literature (28% vs 1–5%). This can be attributed to referral bias where subjects with sternal infection were more often referred for PET imaging. In addition, the gestalt interpretation was performed in consensus, a practice infrequently employed at most imaging centers. Another limitation is the fact that we used subjects without clinical suspicion of SWI as controls, that is, most subjects without SWI were referred for indications other than infection, which can lead to overestimation of the specificity of the test.

Conclusion

FDG-PET/CT may be a useful test for the diagnosis of SWIs. This study suggests that interpretation based on imaging patterns is associated with improved specificity in the recent surgery settings. We have presented an imaging score based on patterns of FDG uptake which can facilitate the interpretation of these studies and allow for accurate diagnosis. However, further validation of this scoring system is required in a larger prospective study.

While diagnosis of SWI based on overall uptake is accurate in the context of remote surgery infections, recent surgery infections should be diagnosed on the basis patterns of uptake as the use of SUV cutoffs limits specifity in these subjects.

Acknowledgments The authors would like to William Leslie for his constructive criticism of the manuscript.

Compliance with Ethical Standards

Conflict of Interest Hadi Hariri, Stéphanie Tan, Patrick Martineau, Yoan Lamarche, Michel Carrier, Vincent Finnerty, Sébastien Authier, Francois Harel, and Matthieu Pelletier-Galarneau declare that they have no conflict of interest.

Ethical Approval This study was conducted in accordance with the ethical standards of the institutional research committee of the Institut de Cardiologie de Montréal (no. 2018-2396).

Informed Consent The requirement to obtain informed consent was waived by our research ethic committee for this retrospective study.

References

1. Filsoufi F, Castillo JG, Rahmanian PB, Broumand SR, Silvay G, Carpentier A, et al. Epidemiology of deep sternal wound infection in cardiac surgery. J Cardiothorac Vasc Anesth. 2009;23:488–94.
2. De Feo M, Renzulli A, Ismeno G, Gregorio R, Della Corte A, Utili R, et al. Variables predicting adverse outcome in patients with deep sternal wound infection. Ann Thorac Surg. 2001;71:324–31.
3. Lazar HL, Vander Salm T, Engelman R, Orgill D, Gordon S. Prevention and management of sternal wound infections. J Thorac Cardiovasc Surg. 2016;152:962–72.
4. Gur E, Stern D, Weiss J, Herman O, Wertheym E, Cohen M, et al. Clinical-radiological evaluation of poststernotomy wound infection. Plast Reconstr Surg. 1998;101:348–55.
5. Yusuf E, Chan M, Renz N, Trampuz A. Current perspectives on diagnosis and management of sternal wound infections. Infect Drug Resist. 2018;11:961–8.
6. Jolles H, Henry DA, Roberson JP, Cole TJ, Spratt JA. Mediastinitis following median sternotomy: CT findings. Radiology. 1996;201:463–6.
7. Akman C, Kantarci F, Cetinkaya S. Imaging in mediastinitis: a systematic review based on aetiology. Clin Radiol. 2004;59:573–85.
8. Quirce R, Carril JM, Gutiérrez-Mendiguchía C, Serrano J, Rabasa JM, Bernal JM. Assessment of the diagnostic capacity of planar scintigraphy and SPECT with 99mTc-HMPAO-labelled leukocytes in superficial and deep sternal infections after median sternotomy. Nucl Med Commun. 2002;23:453.
9. Liberatore M, Fiore V, D'Agostini A, Prosperi D, Iurilli AP, Santini C, et al. Sternal wound infection revisited. Eur J Nucl Med. 2000;27:660–7.
10. Papós M, Nehéz I, Simonfalvi I, Kovács G, Csernay L, Pávics L. Diagnostic value of 99mTc-HM-PAO leukocyte scintigraphy and computer tomography in patients with sternal wound infections. Nucl Med Rev Cent East Eur. 2000;3:35–9.
11. Stumpe KDM, Nötzli HP, Zanetti M, Kamel EM, Hany TF, Görres GW, et al. FDG PET for differentiation of infection and aseptic loosening in total hip replacements: comparison with conventional radiography and three-phase bone scintigraphy. Radiology. 2004;231:333–41.
12. Termaat MF, Raijmakers PGHM, Scholten HJ, Bakker FC, Patka P, Haarman HJTM. The accuracy of diagnostic imaging for the assessment of chronic osteomyelitis: a systematic review and meta-analysis. J Bone Joint Surg Am. 2005;87:2464.
13. Brown TL, Spencer HJ, Beenken KE, Alpe TL, Bartel TB, Bellamy W, et al. Evaluation of dynamic [18F]-FDG-PET imaging for the detection of acute post-surgical bone infection. PLoS One. 2012;7:e41863.
14. Hanley JA, McNeil BJ. A method of comparing the areas under receiver operating characteristic curves derived from the same cases. Radiology. 1983;148:839–43.
15. Read C, Branford OA, Verjee LS, Wood SH. PET-CT imaging in patients with chronic sternal wound infections prior to reconstructive surgery: a case series. J Plast Reconstr Aesthet Surg. 2015;68:1132–7.
16. Zhang R, Feng Z, Zhang Y, Tan H, Wang J, Qi F. Diagnostic value of fluorine-18 deoxyglucose positron emission tomography/computed tomography in deep sternal wound infection. J Plast Reconstr Aesthet Surg. 2018;71(12):1768–76.
17. Gordon BA, Flanagan FL, Dehdashti F. Whole-body positron emission tomography: normal variations, pitfalls, and technical considerations. AJR Am J Roentgenol. 1997;169:1675–80.
18. Kälicke T, Schmitz A, Risse JH, Arens S, Keller E, Hansis M, et al. Fluorine-18 fluorodeoxyglucose positron emission tomography in infectious bone diseases: results of histologically confirmed cases. Eur J Nucl Med. 2000;27:524–8.
19. Ertay T, Sencan Eren M, Karaman M, Oktay G, Durak H. 18F-FDG-PET/CT in initiation and progression of inflammation and infection. Mol Imaging Radionucl Ther. 2017;26:47–52.
20. Mumme T, Reinartz P, Alfer J, Müller-Rath R, Buell U, Wirtz D. Diagnostic values of positron emission tomography versus triple-phase bone scan in hip arthroplasty loosening. Arch Orthop Trauma Surg. 2005;125:322–9.
21. Zhuang H, Duarte PS, Pourdehnad M, Maes A, Acker FV, Shnier D, et al. The promising role of 18F-FDG PET in detecting infected lower limb prosthesis implants. J Nucl Med. 2001;42:44–8.
22. Chacko T, Zhuang H, Stevenson K, Moussavian B, Alavi A. The importance of the location of fluorodeoxyglucose uptake in periprosthetic infection in painful hip prostheses. Nucl Med Commun. 2002;23:851–5.
23. Zhuang H, Chacko TK, Hickeson M, Stevenson K, Feng Q, Ponzo F, et al. Persistent non-specific FDG uptake on PET imaging following hip arthroplasty. Eur J Nucl Med Mol Imaging. 2002;29:1328–33.